4

Characterization of properties and damage in piezoelectrics

Guillermo Rus, Roberto Palma and Javier Suárez
Dept. Structural Mechanics and Hydraulic Engineering, University of Granada
Spain

1. Introduction

The aim of this chapter is to review the state of the art of the possibilities and existing knowledge on characterization of mechanical and coupling properties and damage detection in piezoelectric ceramics. To address the theoretical problem with a proper rational basis, a review of numerical and experimental techniques to solve the so-called inverse problem of characterization of properties and damage is given. Finally, the relevant details of finite element and boundary element formulations and implementation when addressing correct damage simulation in piezoelectric ceramics (Pérez-Aparicio et al. (2007)) is presented.
In recent years, the theoretical framework of inverse problems has been developed to understand and formalize the property and damage characterization problems. This theory has been applied in a variety of continuum mechanics applications, by the groups of Liu & Chen (1996), Oh et al. (2005), Pagano (1970), Rus et al. (2005) and Tarantola & Valette (1982). There is a growing body of knowledge in identification inverse problems for elasticity, like the groups of Tardieu & Constantinescu (2000) or Bonnet & Constantinescu (2005), but due to the intrinsic coupling of magnitudes, the formulation of the piezoelectric problems is more complex than in elastic problems. Despite this difficulty, the electric field and its coupling with the elastic field has the potential to be exploited in monitoring piezoelectrics and in the solution of the inverse problem. Inverse problem techniques have been applied specifically for the piezoelectric ceramics for:

Characterization of properties: The basic formulation has been established by Kaltenbacher et al. (2006) defining a cost functional as the difference between electric impedances observed in laboratory and those obtained after solving the direct problem by the finite element method. A similar cost functional was used by Ruíz et al. (2004a;b), which was minimized using genetic algorithms. On the other hand, Araújo et al. (2006); Araújo et al. (2002) proposed an inverse problem to obtain the constitutive properties of composite plate specimens with surface bonded piezoelectric patches or layers, where the cost functional was the difference between the experimental and FEM–predicted eigen–frequencies and its minimization was carried out using two strategies: a gradient–based method, and neural networks. A genetic algorithm was applied by Chou & Ghaboussi (2001) and Mares & Surace (1996) to solve the IP in elastic structures. Based on crystallographic criteria by Russell & Ghomshei (1997) a cost functional was formulated as the difference in the orientation distribution function, which provides a statistical description of the orientation.

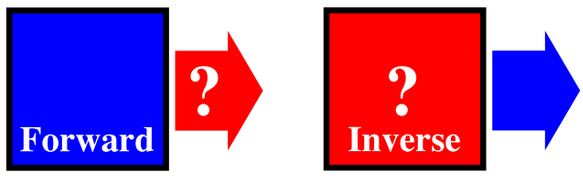

Fig. 1. Inverse problem concept

Damage detection: The group of Palma et al. (2009); Rus et al. (2009) developed the identification inverse problems to design self-diagnosing piezoceramics, by formulating and solving the defects identification problem in piezoelectric plates. They obtained the optimal experimental configuration based on the concept of the probability of detection. Their findings show which excitation-measurement combination provides the most robust self-diagnosis design, and also give criteria to determine which degree of uncertainty needs to be assured in each constitutive property to yield a robust and sensitive damage characterization. A small body of research groups is currently emerging both in the experimental and theoretical fields of monitoring damage in piezoelectrics.

2. Inverse Problems

An Inverse Problem (IP) can be defined in opposition to the forward problem. If a forward problem aims at finding the response (output, in red colour, Fig. 1) of a system given a known model (input, in blue colour), an inverse problem consists in retrieving unknown information of the model given the response as known input data. IPs have been recently applied to study and characterize not only damage or mechanical properties of piezoelectric and classical materials, but provide the general framework for reconstructing an unknown part of a system model.

The model-based IP is the most advanced approach for IP solution. Following Fig. 2, it consists in (1) obtaining a set of experimental measurements given a specific experimental design, which interrogate the system by propagating some physical magnitude that interacts with the unknown part of the system and manifests on an accessible part of it. Some physical assumptions need to be made to generate a mathematical model (2) that can be solved computationally, in which the unknown part of the model to be reconstructed is dependent on some defined parameters. This model simulates the measurements given a set of parameter values. A discrepancy (3) between experimenental and simulated measurements is defined using some metrics to define a Cost Function (CF). The IP is finally solved by finding the values of the parameters that minimize the CF (4), and thus the problem is mathematically fully stated.

Inverse problems are ill-conditioned problems, in the sense that the solution may not be unique, may not exist and may be unstable and divergent. This ill-conditioning is rooted in the physical meaning of the problem, and cannot be completely avoided by purely mathematical manipulations. Instead, some physical pieces of a priori information have to be incorporated into the formulation. This is the basis of a set of techniques called regularization that were formally introduced by Tikhonov & Arsenin (1979); Tikhonov & Arsénine (1974) and extended by Menke (1984) and Aster et al. (2005). These strategies were successfully incorporated to the model-based inverse problem by Rus, establishing a corps of knowledge to be used in this project, while dealing with a variety of mechanical parameter extraction ranging from continuum damage Lee et al. (2007; 2008); Rus & Gallego (2002); Rus & García-Martínez

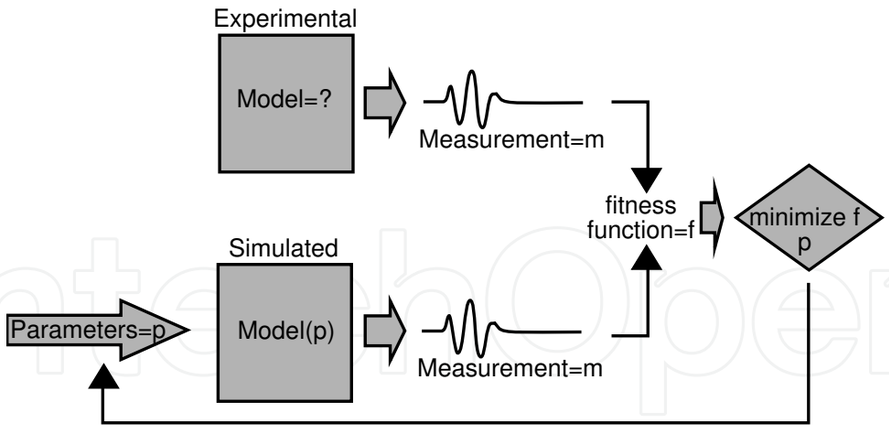

Fig. 2. Model-based inverse problem flowchart

(2007); Rus et al. (2005; 2004) to fractures Gallego & Rus (2004); Rus & Gallego (2005; 2006); Rus et al. (2007a;b) in advanced materials, and using either advanced finite element (FEM) and boundary element (BEM) formulations for the model solution.

2.1 Cost function

The CF, also called objective function, is usually defined (Eqn. 1) as a L-2 norm of the difference between the experimental measurements ψ^{EXP} and those simulated by the numerical procedure ψ^{NUM}, and integrated over the observed period of time T, in the case of dynamic measurements,

$$f = \frac{1}{2NT} \int_T \sum_{i=1}^{N} \left(\psi_i^{EXP} - \psi_i^{NUM} \right)^2 dt \tag{1}$$

Other alternatives are possible, like L-1 norm, or defining the residual between the frequency-domain counterpart of the measurement, or in any other domain.
When genetic algorithms or other heuristic search algorithms are used as for the minimization, an alternative form of the CF is defined, that improves the convergence of the algorithm, as argued by Gallego & Rus (2004),

$$f^L = -\lg\left(f + \varepsilon\right) \tag{2}$$

where ε is a small adimensional constant (typically $\varepsilon = 10^{-16}$) that ensures the existence of the logarithm when f vanishes.

2.2 Parametrization

In the context of inverse problems, parametrization of the model means to characterize the sought solution (the defect in this case) by a set of parameters p_i, which are the working variables and the output of the inverse problem. The choice of parametrization is not obvious, and it is a critical step in the problem setup, since the inverse problem is a badly conditioned one, in the sense that the solution may not be stable, exist or be unique, and the assumptions on the damage model that allow to represent it by a set of parameters can be understood as a strong regularization technique. In particular, a reduced set of parameters is chosen to facilitate the convergence of the search algorithm, and they are also defined to avoid coupling between them.

Typical parametrizations in damage location parameters are some geometric parameters that define the damage extent or size (Level-2 NDE, severity, while Level-1 NDE classification is attained by telling if there is or not damage), other parameters for damage location (Level-3 NDE, location). On the other hand, typical material constant parametrization contain the mechanical, electrical and piezoelectrical constants as coordinates of the parameter vector.

2.3 Search algorithm

The CF minimization can be performed by two alternative families of methods: gradient based methods (among which Gauss-Newton algorithms, BFGS or Simulated annealing are some of the most popular, see Dennis & Schnabel (1983, 1996)) and random search algorithms (Genetic Algorithms, See Goldberg (1989), particle sworm algotihms, simulated annealing, etc.). The latter family require significantly small amount of data in dealing with complex problems, while attaining global convergence as opposed to gradient-based methods, which in opposition are much less computationally expensive.
The IP can be mathematically formalized as a minimization problem, that starts from a measuring system from which the response is recorded, a computational idealization of the system that simulates the measurements (forward problem) depending on the unknown characterization of the defect (parametrization) and defining a CF as above. The solution of the IP is obtained by solving,

$$\min_{p_i} f(p_i) \tag{3}$$

3. Damage characterization

Piezoelectric ceramics are brittle and susceptible to fracture: the ultimate strength is less than 100 [MPa], while the fracture toughness is between 0.5 and 2.0 [MPa/m$^{1/2}$]. Furthermore, due to their ceramic nature, these materials are highly inhomogeneous, causing cracks and/or cavities in the manufacturing process or during their operation. When this occurs, high stress and electric fields concentrations appear around the defect, failing to serve the function for which their were designed. This has contributed to the emergence of many analytical and experimental works about fracture mechanics in the last two decades. However, there are few studies about damage detection, despite it is an interesting way to prevent the failure of these ceramics.
This section describes the damage effects from an analytical and an experimental point of view. Furthermore, inverse problems applied to damage characterization are supervised. Finally, the probability of detection is presented, which gives an idea of the probability that a defect is positively detected, is defined.

3.1 Damage effects: analytical

Analytical studies about piezoelectric fracture mechanics began in 1976 by Parton. Thereafter, traditional mathematical methods, as *Lekhnitskii* and *Stroh* formalisms, used in elastic fracture mechanics were applied to these ceramics. Note that fracture behavior of a piezoelectric ceramic under combined electro-mechanical loading is much more complex than that of the traditional ceramics.

3.1.1 Boundary conditions on defect faces

Several researchers have published theoretical studies on infinite piezoelectric ceramics containing an elliptic hole and have reported different results depending on the electric boundary

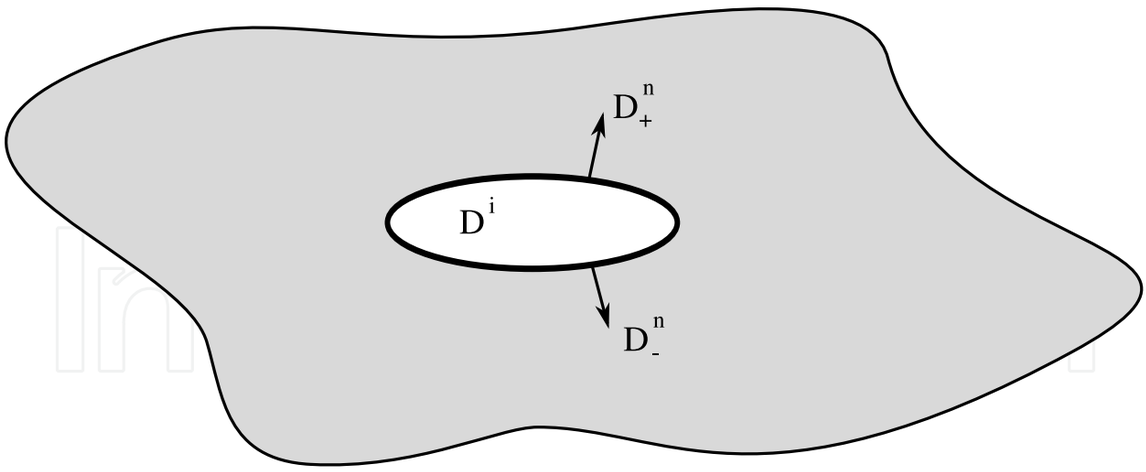

Fig. 3. Normal electric displacement on boundary faces

conditions chosen on defect faces. Therefore, one of the key problems in piezoelectric fracture mechanics is the selection of electric boundary conditions, as it it reported by Ou & Chen (2003).

Consider an infinite piezoelectric ceramic material with a elliptical hole inside, where $\mathbf{D}_{+}^{n}$ and $\mathbf{D}_{-}^{n}$ are the normal electric displacement to upper and lower defect faces, respectively, and $\mathbf{D}^{i}$ is the electric displacement inside the cavity, see Figure 3. There exist three (four for some authors) electric boundary conditions:

Impermeable The dielectric permittivity inside the cavity is assumed to be zero, because it is three order of magnitude less than the ceramic permittivity:

$$\mathbf{D}_{+}^{n} = \mathbf{D}_{-}^{n} = 0 \tag{4}$$

Permeable The dielectric permittivity inside the cavity is assumed to be infinity or, alternatively, both sides of the defect is in electrical contact:

$$\mathbf{D}_{+}^{n} = \mathbf{D}_{-}^{n} \tag{5}$$

Exact This boundary condition is also denominated semi–permeable. It is the only one with physical sense, since the cavity is assumed to behave like a capacitor, from an electrical point of view.

Ou & Chen (2003) reported that: i) impermeable boundary condition has no physical meaning and when it is applied, mathematical singularities appear and ii) permeable boundary condition can be applied when free traction on defect face is assumed. Therefore, the exact boundary condition is the only physically correct and should always be used.

3.1.2 Lekhnitskii formalism–based approach

A 3–D analytical work was developed by Sosa & Pak (1990) in order to study the fracture mechanics of a transversely isotropic ceramic with a crack inside, under electro–mechanics loads. Two important conclusions were obtained:

i) Field variables at crack tip depend on the crack orientation

ii) Crack growth can be accelerated or delayed, depending on the direction of the electric field applied.

Sosa & Pak (1990) only computed the crack tip concentrations, so Sosa (1991) considered an infinity plain strain ceramic with an elliptic hole perpendicular to the polarization direction inside, in order to obtain the field variables around the cavity. Xu & Rajapakse (1999) extended this work considering an arbitrarily oriented elliptic hole and concluding that the highest concentrations occur when the elliptical hole is 33° respect to the polarization direction. In both works was concluded that the stress concentrations at crack tip are higher in piezoelectric than that in anisotropic materials without coupling.
Sosa (1992) used the result obtained by Sosa (1991) to define the intensity factors for piezoelectric ceramics:

$$K_I = \sqrt{a}\, T_{zz}^{\infty} \quad ; \quad K_{IV} = \sqrt{a}\, D_z^{\infty} \tag{6}$$

where a the length of the crack and T_{zz}^{∞} and D_z^{∞} are the stress and electric displacement (fracture mode I) applied, respectively. Note that an electric intensity factor K_{IV} is emerged in piezoelectric materials, in order to compute the electric contribution to the fracture.
In previous works, the impermeable boundary condition is assumed. Sosa & Khutoryansky (1996) applied the exact boundary conditions to expand the study developed by Sosa (1991), concluding that the impermeable boundary condition is unacceptable when the elliptic hole tends to a crack. The same conclusion was numerically obtained by Pérez-Aparicio et al. (2007), using the finite element method. Finally, Hao & Shen (1994) applied the exact boundary condition to obtain the fracture parameters, which were obtained by Sosa (1992) considering the impermeable boundary condition. Then, the fracture parameter of equation (6) are modified by:

$$K_I = \sqrt{\pi a}\, T_{zz}^{\infty} \quad ; \quad K_{IV} = \sqrt{\pi a}\, \left(D_z^{\infty} - D_z^{i} \right) \tag{7}$$

where D_z^i is the electric displacement inside the cavity. Stress intensity factors are not affected by the electric boundary condition. However, the new electric intensity factor K_{IV} depends on the mechanical load applied.

3.1.3 Stroh formalism–based approach

Suo et al. (1992) extend the *Stroh* formalism to piezoelectric problems, considering a semi–infinite piezoelectric ceramics with a crack inside. Plain strain assumption and impermeable boundary condition were assumed to calculate field concentrations and intensity factors. Furthermore, in this work was calculated the energy release rate G_I, which was divided into mechanical G_I^M and electrical parts by Park & Sun (1995a):

$$G_I^M = f\left[(T_{zz}^{\infty})^2 \right] \quad ; \quad G_I = f\left[(T_{zz}^{\infty})^2, T_{zz}^{\infty} D_z^{\infty}, (D_z^{\infty})^2 \right] \tag{8}$$

According to Park & Sun (1995a), the mechanical energy release rate G_I^M has to be used as fracture criteria. However, Gao et al. (1997) and McMeeking (2001) argued that electro–mechanical behaviors can not be studied by fracture mechanical parameters. Therefore, McMeeking (2004) and Wang & Sun (2004) obtained the energy release rate considering the exact boundary condition.

3.2 Damage effects: experimental

Experimental works about piezoelectric fracture mechanics started in 1980, in order to find a fracture criteria for these materials. Two experimental devices are generally used: *Compact Tension* (CT) and *Three Point Bending* (TPB).

Park & Sun (1995b) performed a CT fracture study, where the specimen was a PZT–4 ceramic with a crack inside, which was perpendicular to the poling direction and the applied electric field. It was published, an experimental curve that plots fracture loads F_c versus applied electric field E_a, observing the fracture dependence on applied electric field: F_c increases when $E_a < 0$ and decreases when $E_A > 0$. Similar results were obtained by Fu et al. (2000) and Soh et al. (2003) using PZT–4 and PZT–5 ceramics, respectively. However, Fu et al. (2000) observed that fracture load decreases for positive or negative electric fields applied for PZT–841. On the other hand, Park & Sun (1995b) and Soh et al. (2003) used the analytical results obtained by Park & Sun (1995a) and Gao et al. (1997), respectively, to conclude that the mechanical energy release rate fitted very well with the experimental results.

Jelitto, Kessler, Schneider & Balke (2005) and Jelitto, Felten, Hausler, Kessler, Balke & Schneider (2005) used a PZT–PIC 151 specimen and a TPB device to perform fracture experiments, publishing fracture criteria based on: intensity factors, mechanical and total energy release rates. From a numerical point of view, the intensity factors and the energy release rates ware calculated by the finite element method and considering the three boundary conditions. Finally, it was concluded that the mechanical energy release is more appropriate as fracture criteria, from an empirical point of view.

3.3 Numerical damage characterization approaches

After revising the existing literature (a full review on analytical and experimental piezoelectric fracture mechanics was performed by Chen & Hasebe (2005) and Schneider (2007), respectively), several conclusions are obtained:

- From an analytical point of view, there is no an electric boundary condition can reproduce the experimental results, which explains why current researching are based on non–linear fracture mechanics.
- From an experimental point of view, there is no unique trend for the fracture load as a function of the electric field. This implies that a general fracture criteria can not be developed, which explains the absence of work on piezoelectric reliability.

Therefore, there are many analytical and experimental works about piezoelectric fracture mechanics. However, there are few studies about damage detection, despite it is an interesting way to prevent the failure of these ceramics. Then, several questions appear to remain open: i) the use of the inverse problem to damage detection, ii) optimal experimental measurement setup for improving the inverse problem solutions, iii) probability of detection, iv) inverse problem sensitivity to system uncertainties, v) main variables responsible for the experimental noise and vi) how can the noise be effectively reduced?. All these questions were resolved by the Non–destructive Evaluation Laboratory of the University of Granada, see Rus (2010), by the publishing works: Rus et al. (2009), Palma et al. (2009) and Rus, García-Sánchez, Sáez & Gallego (2010a). Nowadays, these woks are being extended in Rus, Palma & Pérez-Aparicio (2010) and Rus, García-Sánchez, Sáez & Gallego (2010b).

Figure 4 shows a typical flow chart of the model–based inverse problem, where two inputs are introduced: i) parametrization is a number of parameters, which characterize the sought damage and are the inverse problem output and ii) experimental measurements. Finally, a

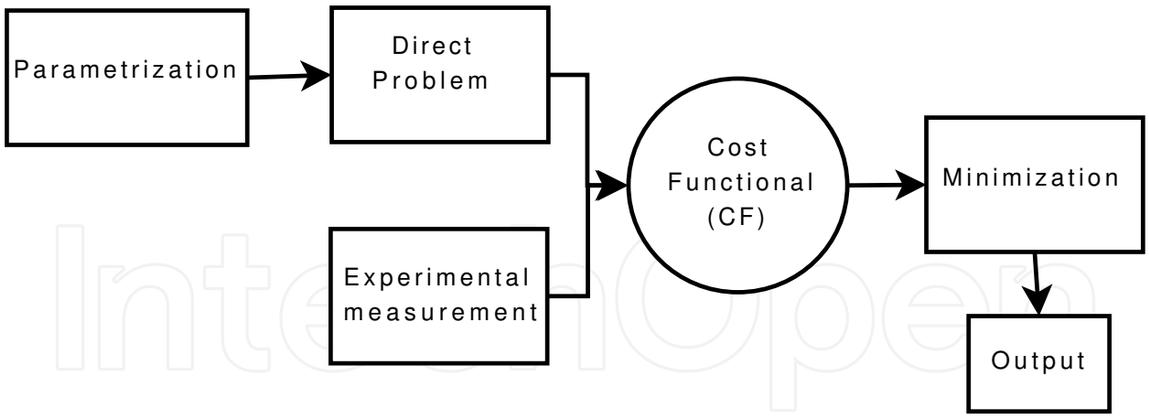

Fig. 4. Flow chart of the model-based inverse problem, see Palma et al. (2009)

cost function is defined and it is minimized by genetic algorithms, as it has been reported in previous sections.

3.3.1 Parametrization

The choice of parametrization is not obvious, and it is a critical step in the problem setup (see Palma et al. (2009)), since the inverse problem is a badly conditioned one, in the sense that the solution may not be stable, exist or be unique, and the assumptions on the damage model that allow to represent it by a set of parameters can be understood as a strong regularization technique. In particular, a reduced set of parameters is chosen to facilitate the convergence of the search algorithm, and they are also defined to avoid coupling between them.
Figure 5 shows a 2D piezoelectric plate of dimensions L_x and L_z with (a) a circular defect or (b) a crack inside, which has to be detected. Note that z is the poling direction. The damage location and size presented suggests the definition of the immediate parameters:

Circular defect $p_i = (x_0, z_0, r)$,

Crack $p_i = (x_0, z_0, L, \theta)$, where L is the length of the crack.

The true (and unknown) parameters are denoted by $\bar{p}_i$. In Rus et al. (2009), Palma et al. (2009) and Rus, Palma & Pérez-Aparicio (2010) a circular defect was considered as a first approximation, to simplify the meshing using the finite element method. On the other hand, in Rus, García-Sánchez, Sáez & Gallego (2010a) and Rus, García-Sánchez, Sáez & Gallego (2010b) a crack was considered, due to the simplicity of the mesh using the boundary element method.

3.3.2 Experimental measurements

Consider the specimen shown in Figure 5 with the circular defect or crack inside. This sample is excited by electrical or mechanical loads, and its response (displacements and/or voltage) is measured at N_i points along the lower boundary of the plate. Note that the piezoelectric coupling makes mechanical loads generate voltages (direct effect) and the electrical loads generate mechanical displacements (inverse effect). On the other hand, the boundary conditions are selected to avoid rigid solid motions.
In the literature there are no works about experimental measurements for damage characterization, so the Non–destructive Evaluation Laboratory of the University of Granada, Rus (2010), is undertaking experimental tests to verify all its numerical results. In Palma et al.

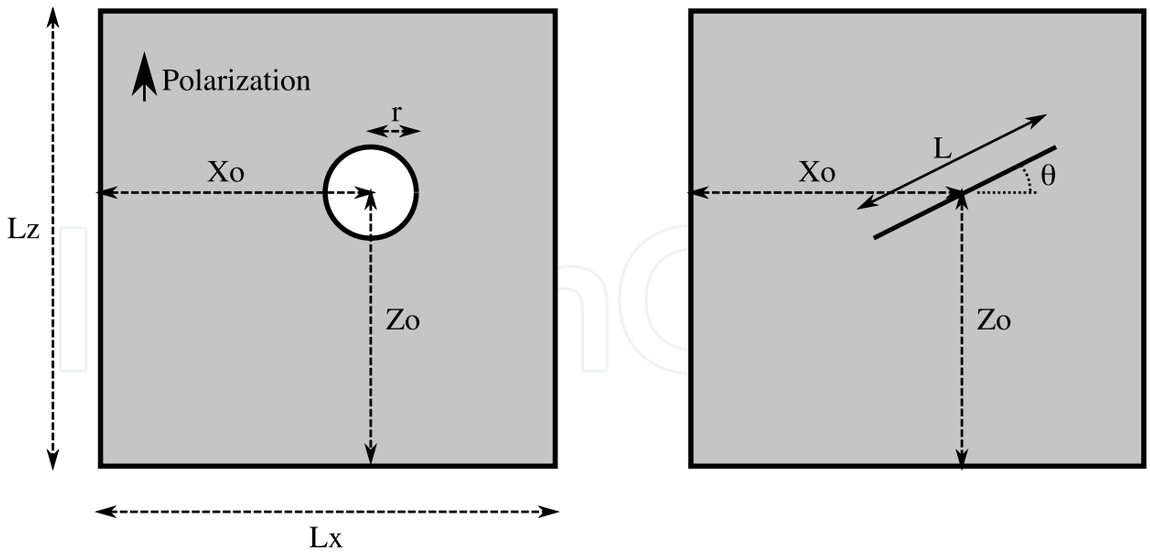

Fig. 5. Piezoelectric plate with (a) a circular defect or (b) a crack inside

(2009); Rus, García-Sánchez, Sáez & Gallego (2010a;b); Rus et al. (2009); Rus, Palma & Pérez-Aparicio (2010) the experimental measurements were generated solving the forward problem by finite or boundary element method and adding noise generated by a gaussian distribution:

$$\psi_i = \psi_i^{FWD} + \xi_i RMS(\psi_i^{FWD})\sigma \tag{9}$$

where ψ_i, ψ_i^{FWD}, ξ_i and σ are the simulated experimental measurements, measurements generated by the solution of the forward problem, random variables, and a parameter defined to study the influence of the noise in the inverse problem solution, respectively. On the other hand, RMS is the root mean square given in Rus et al. (2009).

3.3.3 Results

Figure 6 shows the dependency of the cost functional on the spatial location of the defect (fixing the size at the real value) for increasing noise levels, see Rus et al. (2009). If no noise is simulated, the cost function shows a clear optimum that the search algorithm is able to find. The shape of the cost function is distorted when the noise level increases.
Figure 7 shows the cost function and genetic algorithm convergence for different noise levels. For the case without noise the full convergence is obtained for less than 200 generations. A larger noise level is associated with slower convergence, probably due to the wavy and fuzzy shapes of the cost functional.

3.4 Probability of detection

The Probability of Detection (POD) gives an idea of the probability that a defect is positively detected, given a specimen, a defect size and some noise and system uncertainty conditions.
The detection and characterization of defects is based on the interpretation of the alterations of the measurements due to the presence of the defect, however uncertainties and system noises also alter these measurements. For this reason, the POD is estimated by the probability that

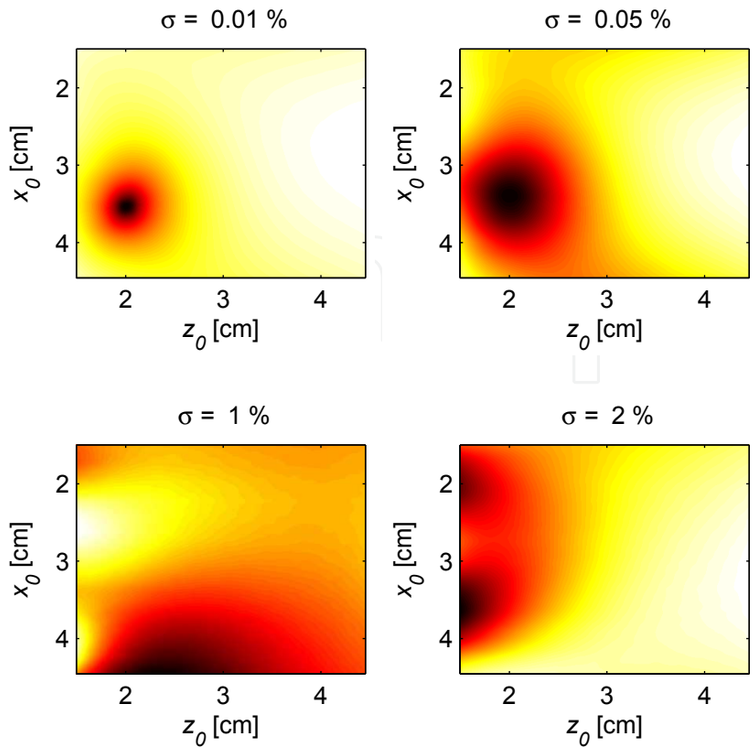

Fig. 6. Cost functional for increasing levels of experimental noise, Rus et al. (2009)

the alteration of the measurement caused by the defect is larger than that caused by the noise, see Rus et al. (2009):

$$\text{POD} = P\left(\frac{|\text{SIGNAL}|^2}{|\text{NOISE}|^2} > 1\right) \tag{10}$$

where SIGNAL and NOISE terms are obtained assuming: i) a linear dependence between the variation of the measurements with increasing noise, see 9 and ii) linear piezoelectric behaviors. Then, the experimental measurements depend on damage area A and noise σ, expanding in *Taylor* series and neglecting higher-order terms:

$$\psi_i(A,\sigma) = \psi_i(0,0) + \underbrace{A\frac{\partial \psi_i}{\partial A}(0,0)}_{\text{SIGNAL}} + \underbrace{\sigma\frac{\partial \psi_i}{\partial \sigma}(0,0)}_{\text{NOISE}} + hot \tag{11}$$

The first term of the right member is the measurement at point i without noise and defect. The second term is the alteration of that measurement due to the presence of the defect only SIGNAL. Finally, the third term is the alteration of the signal originated by the noise only NOISE.

Finally, in Rus et al. (2009) is obtained and validated, using *Monte Carlo* techniques, an analytical expression of the POD, which allows to estimate a priori the minimum defect findable given a specimen geometry and a noise level on measurements.

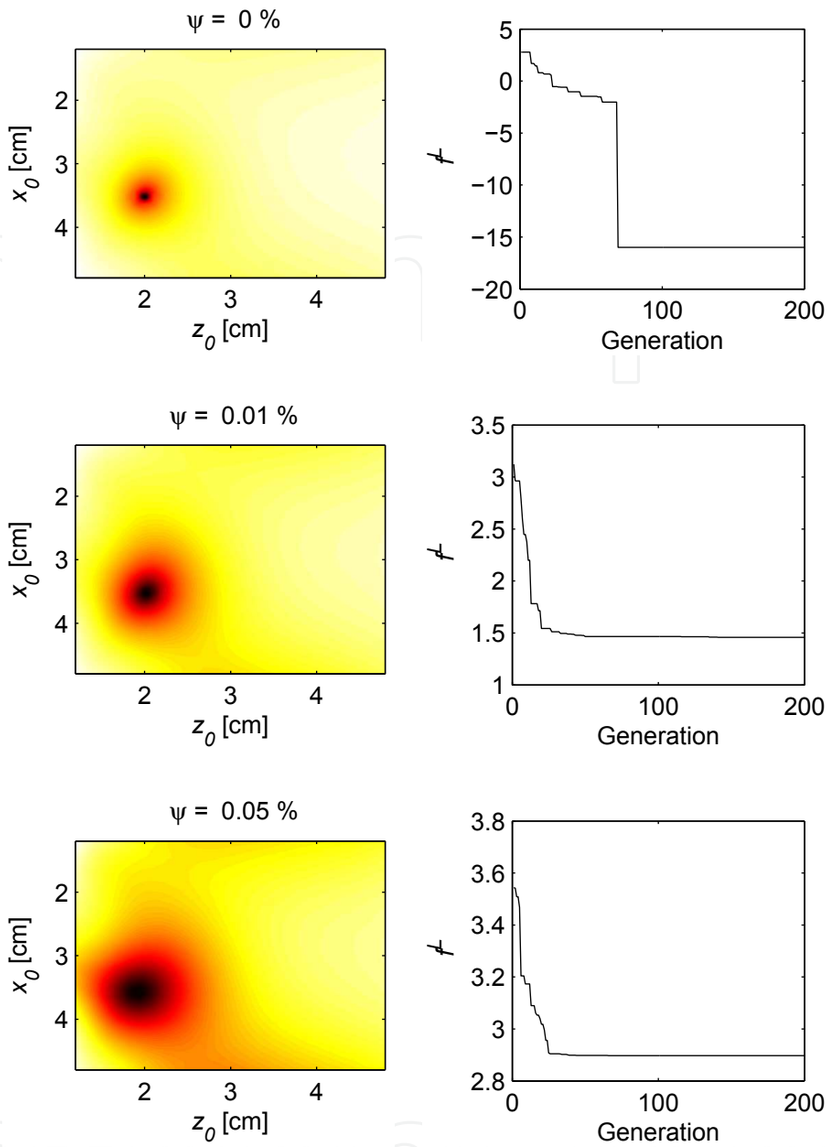

Fig. 7. Cost Function and Genetic Algorithm convergence for different noise levels, see Palma et al. (2009)

4. Property characterization

The performance as sensors or as actuators of piezoelectric elements, usually manufactured in the form of thin films, is defined by the piezoelectric properties, responsible of the electromechanical coupling, but also on the mechanical and electrical properties. These properties need to be established at the material design stage. However, when using piezoelectric crystals for simulation and active noise and vibration control applications, The properties obtained through manufacturer data are in most of the cases not enough to predict the structural be-

haviour and implement effcient control algorithms due to non-homogeneities in materials, and differing geometries and material properties in the regions of actuators and sensors.

4.1 Experimental procedures

Characterization of piezoelectric constants can be based on either the direct or the converse piezoelectric effect. In direct measurements the voltage produced by an applied stress is measured; in indirect measurements the displacement produced by an applied electric field is measured through different methods. The direct measurements can be performed either quasi-statically or dynamically. The first is typically used for nonresonant applications (sensors and actuators), while the second is typical for those applications where the piezoelectric thin film is used for the generation or detection of high-frequency bulk acoustic waves or surface acoustic waves. Various methods have been described for the measurement of the piezoelectric coefficients (see Fig. 8. For instance, the longitudinal piezoelectric coefficient d_{33} (see section 5.1) is determined from the generated charge measured when a calibrated stress is applied to the piezoelectric film.

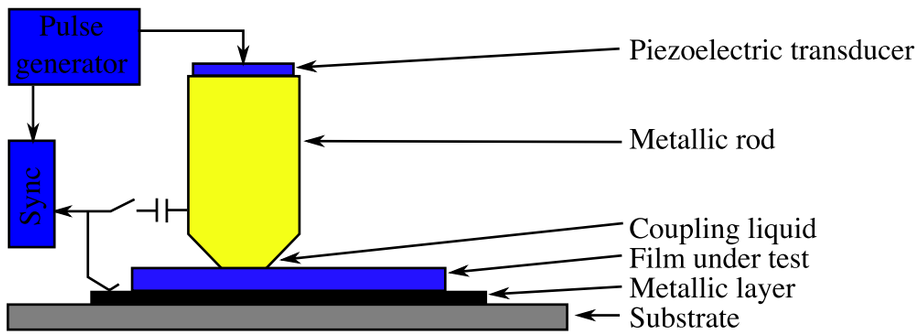

Schematic device for d_{33}characterization

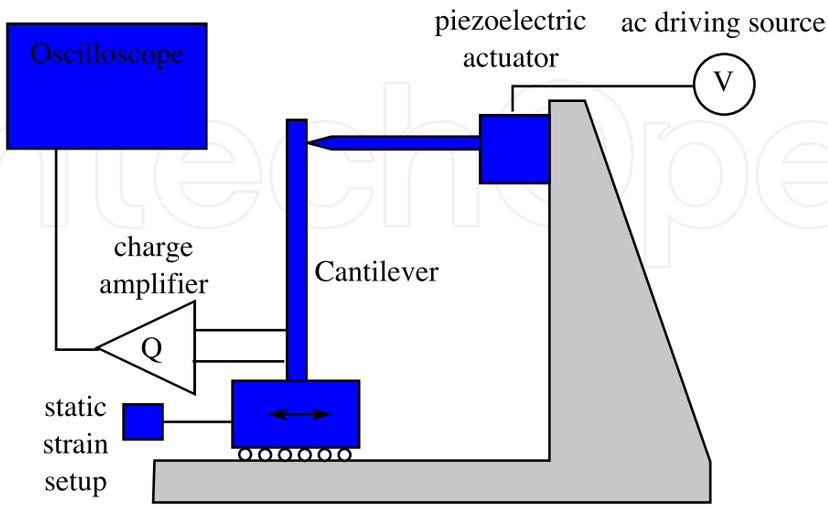

Schematic device for d_{13}characterization

Fig. 8. Experimental setups for constitutive property characterization

A recent and more sophisticated alternative method is based on the Atomic Force Microscopy (AFM), in which a variety of excitation-measurement configurations is applied in order to minimize the effect of the applied electric field with the microscope tip. The evaluation of the transverse e_{31} constant requires different techniques. Here the film is deposited on a cantilever beam and two electrodes are deposited on the free film surface. The free edge of the cantilever is first statically displaced, causing a bending of the cantilever, and then it is suddenly released. The consequent damped oscillation of the cantilever at its natural frequency can be revealed through the voltage appearing between the electrodes and displayed on an oscilloscope. It is proved that the first maximum of the damped oscillation is proportional to the e_{31} constant.
On the other hand, the measurement of the dielectric constants is usually performed with a standard impedance meter.
The complete characterization of piezoelectric constants requires the elastic stiffness coefficients. These can be determined from Surface Acoustic Wave (SAW) velocity dispersion curves that can be obtained in several ways. One method consists of measurement of the phase velocity of several vibration modes. Due to the small amplitude of the vibration, contact-less vibration measurements are usually employed, such as laser interferometry or reflection angle measurement.

4.2 Numerical characterization approaches

When a mathematical model of the piezoelectric system dynamics behaviour of the elements is needed, the physical constants that define the general constitutive laws (see section 5.1) need to be estimated, and this is done by through fit-to-data techniques. The inverse problem is the general theoretical and algorithmic framework to be applied, and in particular, the model-based inverse problem.
To address the limitations of current characterization methods in determining elastic and piezoelectric constants (Araújo et al. (2009); Araújo et al. (2002)) propose a finite element model-based, associated to gradient optimisation-based inverse problem algorithm using vibration data to carry out the identification of electromechanical properties in composite plate specimens with surface bonded piezoelectric patches or layers. This method has been later refined with neural networks to aid the inversion algorithms Araújo et al. (2006).
The problem of how to define which measurements and how to measure in order to minimize the uncertainties of material parameters given the unavoidable measurement noise has recently been addressed by Lahmer et al. (2010). An approach for a similar question based on the definition and maximization of the probability of detection was also addressed by Palma et al. (2009).

4.3 Experimental advances

A few experimental studies regarding the estimation of parameters in mathematical models for homogeneous beams (Banks et al. (1994)), plates and grid structures (Banks & Rebnord (1991)) have been reported. A primary concern when estimating parameters is that the model fits to data consistently across experiments after a time-domain inverse problem solution, for example in the presence of passive damping or for a range of eigenfrequencies (Banks et al. (1997)), to ensure the effectiveness of the model independently of the number of excited frequencies.
Using conventional methods to determine the elastic and piezoelectric constants faces some difficulties in engineered crystals with high coupling constants. The piezoelectric coeffcients

e_{33} and e_{31} (see section 5.1) become unstable using standard methods because they are highly sensitive to the elastic stiffness coefficients c_{12} and c_{13} due to the large d_{31} and d_{33}, yielding serious property fluctuations from sample to sample that often make it impossible to obtain self-consistent data. The derived values of s_{11}, s_{33}, s_{12} and s_{13} also become too sensitive to the variation of c_{13} when its value is close to those of c_{11} and c_{33}. A reversed strategy was suggested by Jiang et al. (2003) using detailed error analysis to determine the best strategy for each given material.

5. Numerical considerations

5.1 Governing equations

Consider a deformable electrically sensitive body, which occupies the region Ω of boundary Γ in a three–dimensional *Euclidean* space, in the absence of electro–mechanical loads.
From a mechanical point of view, the equilibrium and compatibility equations are given by, see Eringen (1980):

$$\nabla \cdot \mathbf{T} + \mathbf{f} = \rho \ddot{\mathbf{u}} \quad ; \quad \mathbf{S} = \nabla^s \mathbf{u} \tag{12}$$

where $\mathbf{T}$, $\mathbf{S}$, $\mathbf{f}$, $\mathbf{u}$ and ρ denote the stress tensor, strain tensor, body forces, displacement and density, respectively. Furthermore, the mechanical boundary conditions are:

$$\begin{aligned} \text{Dirichlet} \quad &\rightarrow \quad \mathbf{u} = \bar{\mathbf{u}} \\ \text{Newmann} \quad &\rightarrow \quad \mathbf{T} \cdot \mathbf{n} = \mathbf{t} \end{aligned} \tag{13}$$

where $\bar{\mathbf{u}}$, $\mathbf{n}$ and $\mathbf{t}$ denote the prescribed displacements, normal unit vector and tractions, respectively.
From an electrical point of view, the governing equations are obtained from the uncoupled *Maxwell* equations, see Eringen & Maugin (1990), and neglecting the free electric charges:

$$\nabla \cdot \mathbf{D} = 0 \quad ; \quad \nabla \times \mathbf{E} = \mathbf{0} \tag{14}$$

where $\mathbf{D}$, $\mathbf{E}$ are the electric displacement or induction and electric field, respectively. According to the fields theory, the induction and the electric field can be obtained from vector $\mathbf{V}$ and scalar ϕ potentials:

$$\begin{aligned} \nabla \cdot \mathbf{D} = 0 \quad &\rightarrow \quad \mathbf{D} = \nabla \times \mathbf{V} \\ \nabla \times \mathbf{E} = \mathbf{0} \quad &\rightarrow \quad \mathbf{E} = -\nabla \phi \end{aligned} \tag{15}$$

This duality allows to define two types of boundary condition, as working with vector or scalar potentials:

$$\begin{aligned} \text{Dirichlet} \quad &\rightarrow \quad \mathbf{V} = \bar{\mathbf{V}} \quad ; \quad \phi = \bar{\phi} \\ \text{Newman} \quad &\rightarrow \quad \mathbf{n} \times \mathbf{E} = \mathbf{E}_s \quad ; \quad \mathbf{n} \cdot \mathbf{D} = D_n \end{aligned} \tag{16}$$

where $\bar{\mathbf{V}}$, $\bar{\phi}$ and D_n are the prescribed electric vector potential, electric scalar potential or voltage and normal electric displacement, respectively, and $\bar{\mathbf{V}} = -\mathbf{n} \times \nabla \phi$.
Finally, the piezoelectric constitutive equations, which couple mechanical and electric fields are given by:

$$\mathbf{T} = \mathbf{c}^E : \mathbf{S} - \mathbf{e}^t \cdot \mathbf{E} \quad ; \quad \mathbf{D} = \mathbf{e} : \mathbf{S} + \boldsymbol{\epsilon}^S \cdot \mathbf{E} \tag{17}$$

where $\mathbf{c}^E$, $\mathbf{e}$ and $\boldsymbol{\epsilon}$ are the elastic, coupling and dielectric material properties, respectively.

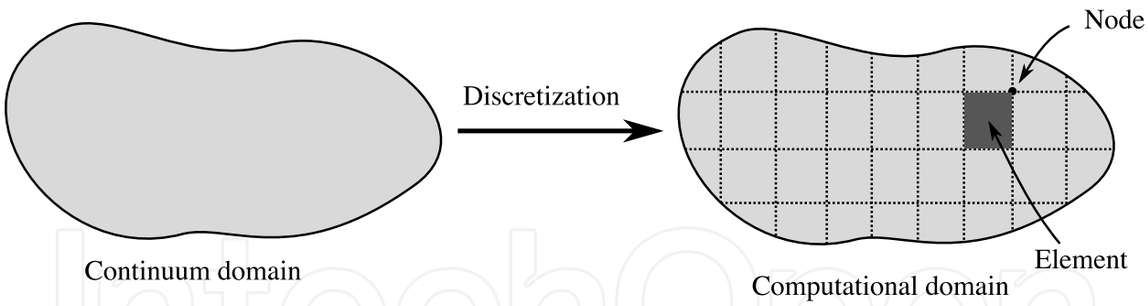

Fig. 9. FEM discretization

5.2 Finite element method

The Finite Element Method (FEM) is a numerical technique for the solution of linear and non–linear partial differential equations, which is used to model many problems in science and engineering. The FEM is the most advanced method for the solution of electro–mechanical field problems, but involves complex mathematical concepts, see Zienkiewicz et al. (2005) or Hughes (1987) for further study. In general, the FEM implies the following steps:

i) The continuum domain Ω is divided into subdomains or elements, which are interconnected at nodal points, see Figure 9.

ii) The nodal values, denominated degrees of freedom, are assumed to be the unknown parameters of the problem.

iii) A set of functions, denominated shape functions, is chose to interpolate the solution within each finite element in terms of its nodal values.

iv) The principle of virtual work is applied to the governing and constitutive equations to obtain the weak form of the problem.

iv) The solution is obtained by solving a set of linear (or non–linear) equations. In order to solve non–linear problems, algorithms such as *Newton–Raphson* has to be applied.

For the piezoelectric problem, two alternative FEM formulations can be developed, according to the equations 15: scalar and vector formulations, which are described in the following sections.

5.2.1 Scalar formulation

The Scalar Formulation (SF) developed in 1970 by Allik & Hughes (1970) has four degree of freedom per node: three displacement and the scalar potential or voltage: $\mathbf{U} = (\mathbf{u}, \phi)^t$, where $(.)^t$ denotes the transpose.

The weak form is obtained applying the principle of the virtual work to the governing equations and constitutive equations. Then, *Newmann* boundary conditions are satisfied automatically, while *Dirichlet* boundary conditions are applied to the nodal values. Subsequently, a discretization is performed using the shape functions $\mathbf{N}$ to interpolate the nodal values $\mathbf{a_u}$ and $\mathbf{a}_\phi$:

$$\begin{aligned} \mathbf{u} = \mathbf{N}\mathbf{a_u} \quad &\rightarrow \quad \mathbf{S} = \mathbf{B}^S\mathbf{a_u} \\ \phi = \mathbf{N}\mathbf{a}_\phi \quad &\rightarrow \quad \mathbf{E} = \mathbf{B}^E\mathbf{a}_\phi \end{aligned} \tag{18}$$

where $\mathbf{B}^S = \nabla^S\mathbf{N}$ and $\mathbf{B} = \nabla \cdot \mathbf{N}$.

Finally, the set of linear equations to be solved is given by:

$$\begin{bmatrix} \mathbf{M} & 0 \\ 0 & 0 \end{bmatrix} \begin{Bmatrix} \ddot{\mathbf{u}} \\ \ddot{\phi} \end{Bmatrix} + \begin{bmatrix} \mathbf{K_{uu}} & \mathbf{K_{u\phi}} \\ \mathbf{K_{\phi u}} & \mathbf{K_{\phi\phi}} \end{bmatrix} \begin{Bmatrix} \mathbf{u} \\ \phi \end{Bmatrix} + \begin{Bmatrix} \mathbf{f_u} \\ \mathbf{f_\phi} \end{Bmatrix} = \begin{Bmatrix} \mathbf{0} \\ \mathbf{0} \end{Bmatrix} \tag{19}$$

where the stiffness matrices are:

$$\begin{aligned} \mathbf{K_{uu}} &= \int_\Omega \mathbf{B}^S \mathbf{c}^E \mathbf{B}^S \mathrm{d}\Omega \quad ; \quad \mathbf{K_{u\phi}} = \int_\Omega \mathbf{B}^S \mathbf{e}^t \mathbf{B}^E \mathrm{d}\Omega \\ \mathbf{K_{\phi u}} &= \int_\Omega \mathbf{B}^E \mathbf{e} \mathbf{B}^S \mathrm{d}\Omega \quad ; \quad \mathbf{K_{\phi\phi}} = -\int_\Omega \mathbf{B}^E \boldsymbol{\epsilon}^S \mathbf{B}^E \mathrm{d}\Omega \end{aligned} \tag{20}$$

the kinematically consistent mass matrix is given by:

$$\mathbf{M} = \int_\Omega \mathbf{B}^S \rho \mathbf{B}^S d\Omega \tag{21}$$

and the body forces vector are:

$$\begin{aligned} \mathbf{f_u} &= -\int_\Omega \mathbf{B}^S \mathbf{f} \mathrm{d}\Omega - \int_\Gamma \mathbf{B}^S \mathbf{t} \mathrm{d}\Gamma \\ \mathbf{f}_\phi &= -\int_\Gamma \mathbf{B}^E \rho_\Gamma \mathrm{d}\Gamma \end{aligned} \tag{22}$$

Note that this formulation is monolithic, that is, the coupling is at the stiffness matrix. In Gaudenzi & Bathe (1995) an iterative (stagger) formulation was proposed, which iteratively solves the mechanical and the electric problems. On the other hand, elastic, coupling and dielectric properties have different orders of magnitude, making extremely ill-conditioned to the stiffness matrix. This drawback was resolved in Qi et al. (1997) by rescaling the dimensions of the properties.
Zeng & Rajapakse (2004) developed a FEM to include the remanent strain and remanent polarization induced by poling. This was the first step to model the hysteresis, which is a non–linear behavior inherent to ferroelectric materials. As it is reported in Kaltenbacher et al. (2010), three different approaches are developed to model the hysteresis, namely: i) thermodynamically consistent models (see, Kamlah & Bohle (2001)), ii) micromechanical models and iii) models with hysteresis operator, see Kaltenbacher et al. (2010).

5.2.2 Vector formulation

The Vector Formulation (VF) was developed by Landis (2002) in 2002. In this formulation there are six degrees of freedom per node (three displacements and three components of the vector potential): $\mathbf{U} = (\mathbf{u}, \mathbf{V})^t$. The discretization, weak form and set of equations are obtained in a similar way to that used in SF. However, the main difference arises choosing the constitutive equations, where the electric displacement has to be chosen such as independent variable for this formulation.
A problem of the VF is the loss of uniqueness. Thus, in Semenov et al. (2006) some gauging procedures were investigated and, finally, the *Coulomb* gauge was incorporated to the FEM formulation, using the penalty function method.

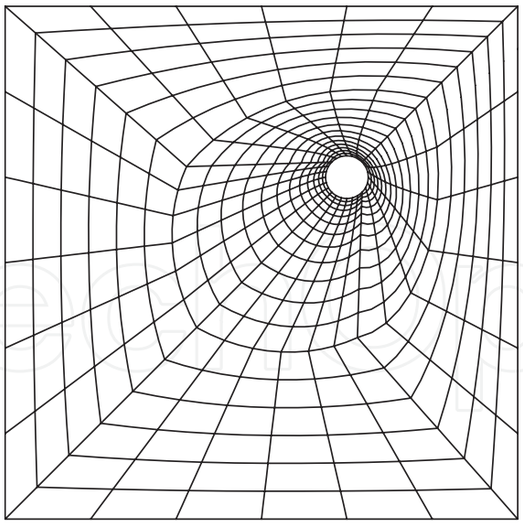

Fig. 10. Optimized mesh for damage detection using the FEM

The main drawback of the VF is the increase of CPU time, because there are six degrees freedom per node (four in the SF). However, this disadvantage can be offset by the rapid convergence in non–linear problems.
In terms of the inverse problem solutions the SF is better than VF, because in the laboratory it is easier to measure voltages than vector potentials, which are a mathematical artifice and not a physical observable.

5.2.3 Mesh generation for damage detection

The mesh generation is the main step to achieve accurate and reliable results using the finite element method. Therefore, Rus et al. (2009) developed an algorithm that automatically generates a high quality mesh. Given a square domain with a random (x_0, y_0, r) circle hole inside (see Figure 5), the fully automatic algorithm to construct multi–block structured 2D meshes consists of three steps:

i) The domain is subdivided into simple blocks by means of medial axis transform, which is the locus of centers of maximal empty circles inside the domain. Therefore, the domain skeleton is obtained in this step.

ii) Blocks are meshed by transfinite interpolation, which is a technique to draw meshes mapping the unit square onto the interior of the physical domain.

iii) Elements are concentrated close to the circular hole using a stretching function, which is a monotonously increasing function defined in the computational domain.

Finally, Figure 10 shows an optimized mesh generated with the previous algorithm, where the maximum element size is selected to provide an error in the measurements below an acceptable threshold, see Rus et al. (2009).

5.3 Boundary element method

The boundary element method is an alternative technique to model the response of piezoelectric materials in the case of linear constitutive laws particularly for three reasons: (1) the dimensionality of the problem is reduced by one in comparison with the FEM, requiring only

boundary meshing instead of domain meshing; (2) the cracks are easily modeled by a single boundary after introducing the so-called hypersingular formulation; and (3) infinite boundary conditions in the case of dynamics are satisfied automatically, without need for infinite finite elements, as is the case for the FEM.
However the formulation of the problem is complex for the case of piezoelectric materials with cracks and has only been accomplished in recent years, for the case of static piezoelectricity, by García-Sanchez et al. (2005); García-Sánchez et al. (2005; 2008) and for transient dynamics by Rojas-Díaz et al. (2009; 2010).

6. Future challenges

Several issues remain unsolved in the fields of damage and material properties characterization in piezoelectrics, which makes it a fertile researh field where concepts from other disciplines may give new insights.
In the case of damage, fracture growth criteria are a controversial issue, since the mechanical, electrical and total energy release rates have inconsistent relationships with crack opening at the theoretical level. The question of the identifiability, or minimal detectable damage, has neither been addressed, except for some preliminar approaches to the concept of probability of detection.
Regarding the property characterization, the established methods have a limited range of validity, and optimal measurement/excitation setups need to be determined and rationally justified. Furthermore, the classical characterization procedures extract some scalar parameters from the measurement, dumping large amounts of data that may contain useful information about the material constants. The complete measurements may be taken advantage of using model-based inverse problems to reconstruct the unknown coefficients of the constitutive model.

7. References

Allik, H. & Hughes, T. (1970). Finite elment method for piezoelectric vibration, *International Journal for Numerical Methods in Engineering* **2**: 151–157.

Araújo, A. L., Soares, C. M. M., Herskovits, J. & Pedersen, P. (2006). Parameter estimation in active plate structures using gradient optimisation and neural networks., *Inverse Prob. in Sci. and Eng.* **5**: 483–493.

Araújo, A., Soares, C. M., Herskovits, J. & Pedersen, P. (2009). Estimation of piezoelastic and viscoelastic properties in laminated structures, *Composite Structures* **87**(2): 168 – 174. US Air Force Workshop Structural Assessment of Composite Structures.

Araújo, A., Soares, C. M., Herskovits, J. & Pedersen, P. (2002). Development of a finite element model for the identification of mechanical and piezoelectric properties through gradient optimisation and experimental vibration data, *Composite Structures* **58**: 307–318.

Aster, R. C., Borchers, B. & Thurber, C. H. (2005). *Parameter Estimation and Inverse Problems*, Elsevier, USA.

Banks, H. T. & Rebnord, D. A. (1991). Estimation of material parameters for grid structures, *Journal of Mathematical Systems, Estimation and Control* **1**: 188–197.

Banks, H. T., Smith, R. C., Brown, D. E., Metcalf, V. L. & Silcox, R. J. (1997). The estimation of material and patch parameters in a pde-based circular plate model, *Journal of Sound and Vibration* **199**(5): 777 – 799.

Banks, H. T., Wang, Y. & Inman, D. J. (1994). Bending and shear damping in beams: frequency domain estimation techniques, *Journal of Vibration and Acoustics* **116**: 188–197.

Bonnet, M. & Constantinescu, A. (2005). Inverse problems in elasticity, *Inverse Problems* **21**: R1–R50.

Chen, Y. & Hasebe, N. (2005). Current understanding on fracture behavior of ferroelectric/piezoelectric materials, *J. Intell. Mater. Syst. Struct.* **16**: 673–687.

Chou, J. & Ghaboussi, J. (2001). Genetic algorithm in structural damage detection, *Comput. Strut.* **79**: 1335–1353.

Dennis, Jr., J. E. & Schnabel, R. B. (1983, 1996). *Numerical Methods for Unconstrained Optimization and Nonlinear Equations*, SIAM, Philadelphia.

Eringen, A. (1980). *Mechanics of Continua*, Robert E. Krieger Publishing Company.

Eringen, A. & Maugin, G. (1990). *Electrodynamics of Continua I*, Springer-Verlag New York, Inc.

Fu, R., Qian, C. & Zhang, T. (2000). Electric fracture toughness for conductive cracks driven by electric fields, *Applied Physics Letters* **76**(1): 126–128.

Gallego, R. & Rus, G. (2004). Identification of cracks and cavities using the topological sensitivity boundary integral equation, *Computational Mechanics* **33**.

Gao, H., Zhang, T. & Tong, P. (1997). Local and global energy release rates for an electrically yielded crack in a piezoelectric ceramic, *Journal of the Mechanics and Physics of Solids* **45**(4): 491–510.

García-Sanchez, F., Sáez, A. & Domínguez, J. (2005). Anisotropic and piezoelectric materials fracture analysis by bem, *Computers & Structures* **83**: 804–820.

García-Sánchez, F., Sáez, A. & Domínuez, J. (2005). Two-dimensional time-harmonic bem for cracked anisotropic solids, *Engineering Analysis with Boundary Elements* .

García-Sánchez, F., Zhang, C. & Sáez, A. (2008). 2-d transient dynamic analysis of cracked piezoelectric solids by a time-domain bem, *Computer Methods in Applied Mechanics and Engineering* **197**: 3108–3121.

Gaudenzi, P. & Bathe, K. (1995). An iterative finite element procedure for the analysis of piezoelectric continua, *Journal of Intelligent Material Systems and Structures* **6**: 266–273.

Goldberg, D. (1989). *Genetic algorithms in search, optimization and machine learning*, Addison-Wesley Publ, Reading, Massachussets, etc.

Hao, T. & Shen, Z. (1994). A new electric boundary condition of electric fracture mechanics and its applications, *Engineering Fracture Mechanics* **47**(6): 793–802.

Hughes, T. (1987). *Th Finite Element Method. Linear Static and Dynamic Finite Element Analysis*, Prentice-Hall, Inc.

Jelitto, H., Felten, F., Hausler, C., Kessler, H., Balke, H. & Schneider, G. (2005). Measurement of energy release rates for cracks in pzt under electromechanical loads, *Journal of the European Ceramic Society* **25**: 2817–2820.

Jelitto, H., Kessler, H., Schneider, G. & Balke, H. (2005). Fracture behavior of poled piezoelectric pzt under mechanical and electrical loads, *Journal of the European Ceramic Society* **25**: 749–757.

Jiang, W., Zhang, R., Jiang, B. & Cao, W. (2003). Characterization of piezoelectric materials with large piezoelectric and electromechanical coupling coefficients, *Ultrasonics* **41**(2): 55 – 63.

Kaltenbacher, B., Lahmer, T., Mohr, M. & Kaltenbacher, M. (2006). Pde based determination of piezoelectric material tensors, *Europ. J. App. Mathem.* **17**: 383–416.

Kaltenbacher, M., Kaltenbacher, B., Hegewald, T. & Lerch, R. (2010). Finite element formulation for ferroelectric hysteresis of piezoelectric materials, *Journal of Intelligent Material Systems and Structures* **21**: 773–785.

Kamlah, M. & Bohle, U. (2001). Finite element analysis of piezoceramic components taking into account ferroelectric hysteresis behavior, *International Journal of Solids and Structures* **38**: 605–633.

Lahmer, T., Kaltenbacher, B. & Schulz, V. (2010). Optimal measurement selection for piezoelectric material tensor identification, *Inverse Problems in Science and Engineering* **16**: 369–387.

Landis, C. (2002). A new finite-element formulation for electromechanical boundary value problems, *International Journal for Numerical Methods in Engineering* **55**: 613–628.

Lee, S. Y., Rus, G. & Park, T. (2007). Detection of stiffness degradation in laminated composite plates by filtered noisy impact testing, *Comp. Mech.* pp. 1–15.

Lee, S. Y., Rus, G. & Park, T. H. (2008). Quantitative nondestructive evaluation of thin plate structures using the complete frequency from impact testing, *Struct. Eng. Mech.* **28**: 525–548.

Liu, P. & Chen, C. (1996). Parametric identification of truss structures by using transient response, *J. Sound Vib.* **191**: 273–287.

Mares, C. & Surace, C. (1996). On application of genetic algorithms to identify damage in elastic structures, *J. Sound Vib.* **195**: 195–215.

McMeeking, R. (2001). Towards a fracture mechanics for brittle piezoelectric and dielectric materials, *International Journal of Fracture* **108**: 25–41.

McMeeking, R. (2004). The energy release rate for a griffith crack in a piezoelectric material, *Engineering Fracture Mechanics* **71**: 1149–1163.

Menke, W. (1984). *Geophysical data analysis, Discrete Inverse Theory*, Academic Press INC.

Oh, J., Cho, M. & Kim, J. (2005). Dynamic analysis of composite plate with multiple delaminations based on higher–order zigzag theory, *Int. J. Solids & Struct.* **42**: 6122–6140.

Ou, Z. & Chen, Y. (2003). Dicussion of the crack face electric boundary condition in piezoelectric fracture mechanics, *International Journal of Fracture* **123**: L151–L155.

Pagano, N. (1970). Exact solution for rectangular bidirectional composites and sandwich plate, *J. Comp. Mater.* **4**: 20–34.

Palma, R., Rus, G. & Gallego, R. (2009). Probabilistic inverse problem and system uncertainties for damage detection in piezoelectrics, *Mechanics of Materials* **41**: 1000–1016.

Park, S. & Sun, C. (1995a). Effect of electric field on fracture of piezoelectric ceramics, *International Journal of Fracture* **70**: 203–216.

Park, S. & Sun, C. (1995b). Fracture criteria for piezoelectric ceramics, *J. Am. Ceram. Soc.* **78**(6): 1475–1480.

Pérez-Aparicio, J., Sosa, H. & Palma, R. (2007). Numerical investigation of field-defect interactions in piezoelectric ceramics, *International Journal of Solids and Structures* **44**: 4892–4908.

Qi, H., Fang, D. & Yao, Z. (1997). Fem analysis of electro-mechanical coupling effect of piezoelectric materials, *Computational Materials Science* **8**: 283–290.

Rojas-Díaz, R., García-Sánchez, F. & Sáez, A. (2009). Dynamic crack interactions in magnetoelectroelastic composite materials, *International Journal of Fracture* **47**: 119–130.

Rojas-Díaz, R., García-Sánchez, F. & Sáez, A. (2010). Analysis of cracked magnetoelectroelastic composites under time-harmonic loading, *International Journal of Solids and Structures* **47**: 71–80.

Ruíz, A., Ramos, A. & San-Emeterio, J. (2004a). Estimation of some transducer parameters in a broadband piezoelectric transmitter by using an artificial intelligence technique, *Ultrasonics* **42**: 459–463.

Ruíz, A., Ramos, A. & San-Emeterio, J. (2004b). Evaluation of piezoelectric resonator parameters using an artificial intelligence technique, *Integrated Ferroelectric* **63**: 137–141.

Rus, G. (2010). Nondestructive evaluation laboratory.
URL: *http://www.ugr.es/local/grus/research.htm*

Rus, G. & Gallego, R. (2002). Optimization algorithms for identification inverse problems with the boundary element method, *Engineering Analysis with Boundary Elements* **26**: 315–327.

Rus, G. & Gallego, R. (2005). Boundary integral equation for inclusion and cavity shape sensitivity in harmonic elastodynamics, *Engineering Analysis with Boundary Elements* **25**: 77–91.

Rus, G. & Gallego, R. (2006). Solution of identification inverse problems in elastodynamics using semi-analytical sensitivity computation, *Engineering Analysis with Boundary Elements* p. in press.

Rus, G. & García-Martínez, J. (2007). Ultrasonic tissue characterization for monitoring nanostructured tio_2-induced bone growth, *Phys. Med. Biol.* **52**: 3531–3547.

Rus, G., García-Sánchez, F., Sáez, A. & Gallego, R. (2010a). Damage detection in piezoceramics via bem, *Key Engineering Materials* **417**: 381–384.

Rus, G., García-Sánchez, F., Sáez, A. & Gallego, R. (2010b). Feasibility of model-based damage identification in piezoelectric ceramics, *In preparation* **-**: –.

Rus, G., Lee, S. & Gallego, R. (2005). Defect identification in laminated composite structures by bem from incomplete static data, *Int. J. Solids and Structures* **42**: 1743–1758.

Rus, G., Lee, S.-Y. & Gallego, R. (2004). Defect indentification in laminated composite structures by BEM from incomplete static data, *ijss* **4**(5-6): 1743–1758.

Rus, G., Palma, R. & Pérez-Aparicio, J. (2009). Optimal measurement setup for damage detection in piezoelectric plates, *International Journal of Engineering Science* **47**: 554–572.

Rus, G., Palma, R. & Pérez-Aparicio, J. (2010). Experimental design of dynamic model-based damage identification in piezoelectric ceramics, *In preparation* **-**: –.

Rus, G., Wooh, S. C. & Gallego, R. (2007a). Processing of ultrasonic array signals for characterizing defects. part i: Signal synthesis, *IEEE T. Ultrason. Ferr.* **october**: 2129–2138.

Rus, G., Wooh, S. C. & Gallego, R. (2007b). Processing of ultrasonic array signals for characterizing defects. part ii: Experimental work, *IEEE T. Ultrason. Ferr.* **october**: 2139–2145.

Russell, R. & Ghomshei, M. (1997). Inverting piezoelectric measurements, *Tectonophysics* **271**: 21–35.

Schneider, G. (2007). Influence of electric field an mechanical stresses on the fracture of ferroelectrics, *Annu. Rev. Mater. Res.* **37**: 491–538.

Semenov, A., Kessler, H., Liskowsky, A. & Balke, H. (2006). On a vector potential formulation for 3d electromechanical finite element analysis, *Communications in Numerical Methods in Engineering* **22**: 357–375.

Soh, A., Lee, K. & Fang, D. (2003). On the effect of an electric field on the fracture toughness of poled piezoelectric ceramics, *Materials Science and Engineering A* **360**: 306–314.

Sosa, H. (1991). Plane problems in piezoelectric media with defects, *International Journal of Solids and Structures* **28**(4): 491–505.

Sosa, H. (1992). On the fracture mechanics of piezoelectric solids, *International Journal of Solids and Structures* **29**(21): 2613–2622.

Sosa, H. & Khutoryansky, N. (1996). New developments concerning piezoelectric materials with defects, *International Journal of Solids and Structures* **33**(23): 3399–3414.

Sosa, H. & Pak, Y. (1990). Three-dimensional eigenfuction analysis of a crack in a piezoelectric material, *International Journal of Solids and Structures* **26**(1): 1–15.

Suo, Z., Kuo, C., Barnett, D. & Willis, J. (1992). Fracture mechanics for piezoelectric ceramics, *Journal of the Mechanics and Physics of Solids* **40**(4): 739–765.

Tarantola, A. & Valette, B. (1982). Inverse problems = quest for information, *J. Geophys.* **50**: 159–170.

Tardieu, N. & Constantinescu, A. (2000). On the determination of elastic coefficients from indentation experiments, *Inverse Problems* **16**: 577–588.

Tikhonov, A. & Arsenin, V. (1979). *Methods for solving ill-posed problems*, Nauka, Moscow.

Tikhonov, A. & Arsénine, V. (1974). *Méthodes de résolution de problémes mal posés*, Editions Mir, Moscou.

Wang, B. & Sun, Y. (2004). Intensity factors for some common piezoelectric fracture mechanics specimens with conducting cracks or electrodes, *International Journal of Engineering Science* **42**: 1129–1153.

Xu, X. & Rajapakse, R. (1999). Analytical solution for an arbitrarily oriented void/crack and fracture of piezoceramics, *Acta Mater.* **47**(6): 1735–1747.

Zeng, X. & Rajapakse, R. (2004). Effects of remanent field on an elliptical flaw and a crack in a poled piezoelectric ceramic, *Computational Materials Science* **30**: 433–440.

Zienkiewicz, O., Taylor, R. & Zhu, J. (2005). *The Finite Element Method: The Basis*, Elsevier Butterworth-Heinemann.

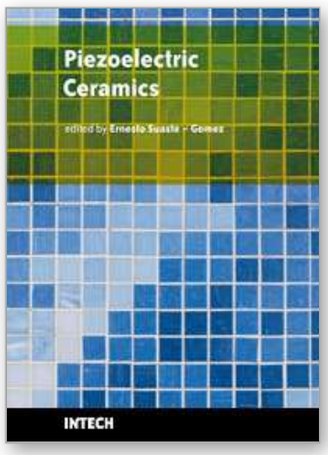

Piezoelectric Ceramics

Edited by Ernesto Suaste-Gomez

ISBN 978-953-307-122-0

Hard cover, 294 pages

Publisher Sciyo

Published online 05, October, 2010

Published in print edition October, 2010

This book reviews a big window of opportunity for piezoelectric ceramics, such as new materials, material combinations, structures, damages and porosity effects. In addition, applications of sensors, actuators, transducers for ultrasonic imaging, positioning systems, energy harvesting, biomedical and microelectronic devices are described. The book consists of fourteen chapters. The genetic algorithm is used for identification of RLC parameters in the equivalent electrical circuit of piezoelectric transducers. Concept and development perspectives for piezoelectric energy harvesting are described. The characterization of principal properties and advantages of a novel device called ceramic-controlled piezoelectric with a Pt wire implant is included. Bio-compatibility studies between piezoelectric ceramic material and biological cell suspension are exposed. Thus, piezoelectric ceramics have been a very favorable solution as a consequence of its high energy density and the variety of fabrication techniques to obtain bulk or thin films devices. Finally, the readers will perceive a trend analysis and examine recent developments in different fields of applications of piezoelectric ceramics.

How to reference

In order to correctly reference this scholarly work, feel free to copy and paste the following:

Guillermo Rus, Roberto Palma and Javier Suárez (2010). Characterization of Properties and Damage in Piezoelectrics, Piezoelectric Ceramics, Ernesto Suaste-Gomez (Ed.), ISBN: 978-953-307-122-0, InTech, Available from: http://www.intechopen.com/books/piezoelectric-ceramics/characterization-of-properties-and-damage-in-piezoelectrics

INTECH
open science | open minds

InTech Europe
University Campus STeP Ri
Slavka Krautzeka 83/A
51000 Rijeka, Croatia
Phone: +385 (51) 770 447
Fax: +385 (51) 686 166
www.intechopen.com

InTech China
Unit 405, Office Block, Hotel Equatorial Shanghai
No.65, Yan An Road (West), Shanghai, 200040, China
中国上海市延安西路65号上海国际贵都大饭店办公楼405单元
Phone: +86-21-62489820
Fax: +86-21-62489821

IntechOpen